JTTEE5 5:154-160

Corrosion Behavior of Aluminum Weld Overlay Alloys with Dispersed Niobium Carbide Particles in Sodium Chloride Solution

Y. Takatani, T. Tomita, K. Tani, and Y. Harada

Aluminum overlay weld alloys with dispersed niobium carbide particles (NbCp/Al) were prepared by a plasma transferred arc welding process. The corrosion behavior of the NbCp/Al alloys was studied in sodium chloride solution by means of electrochemical techniques and scanning electron microscopy. The aluminum alloys under investigation were pure aluminum, aluminum-magnesium, aluminum-magnesium-silicon, and aluminum-copper. The addition of NbC particles shifted the corrosion potentials in the positive direction. However, the pitting potentials were almost similar to that of overlay weld alloy without NbC particles. In the immersion test in quiescent 0.5 *M* NaCl open to the air, preferential localized corrosion of all NbCp/Al alloys was observed at the matrix between NbC particles and crystalline phases.

1. Introduction

SURFACE HARDENING of soft aluminum alloys adds desirable wear resistance. In a hard surfacing process, a relatively hard coating in a layer about 3 mm thick is applied to the soft substrate (Ref 1). In forming this type of thick hard surfacing, one effective approach is the plasma transferred arc welding (PTA) method (Ref 2), which uses a plasma arc as a heat source. This method is used in practice in the overlay welding of steel. In other words, in the PTA method, hard carbide particles are distributed on the aluminum alloy, forming a carbide particle dispersion overlay weld layer that hardens the surface (Ref 3, 4).

The aluminum alloy matrix composites with the dispersed carbides are strong and have superior mechanical properties such as wear resistance. Silicon-carbide/aluminum composite is expected to be adapted for practical use (Ref 5). However, to make these composites and overlay weld alloys practical, it is necessary to be aware of their chemical properties, such as their ability to withstand corrosion in aqueous solution. There have been several reports on the corrosion of carbide-strengthened aluminum alloy matrix composites (Ref 6-12). These reports have assessed several key forms of corrosion, including corrosion of the carbide or of the metal itself, galvanic corrosion due to the presence of other materials, corrosion caused by formation of compounds at the carbide-matrix interfaces, and crevice corrosion at the pores and crevices along the carbide-matrix interfaces. However, none of these reports have clarified the corrosion behavior of these composites.

In this study, overlay weld layers were created by dispersing NbC carbide particles onto various aluminum alloys using the PTA method. The corrosion resistance of the NbC particle dispersion overlay weld alloys in sodium chloride solution was then evaluated and the corrosion behavior of the carbide/metal matrix composites was investigated.

Keywords aluminum alloy, electrochemical measurement, niobium carbide, overlay weld alloy, plasma transferred arc welding process, sodium chloride

Y. Takatani, Hyogo Prefectural Institute of Industrial Research, Yukihira-cho, Suma-Ku, Kobe, 654, Japan; **T. Tomita,** Hyogo Prefectural Institute of Industrial Research, Azafuke, Hirata, Miki, 673-04, Japan; **K. Tani** and **Y. Harada,** Tocalo Co., Ltd., Fukaekita-Machi, Higashinada-Ku, Kobe, 658, Japan.

2. Experimental Method

2.1 *Production of Overlay Weld Alloys*

Niobium carbide powder with particles measuring 60 to 150 μm was dispersed in the overlay weld alloy. As shown in Table 1, four aluminum alloy substrates were used: 99.99 mass% Al (4NAl), aluminum-magnesium (5052Al), aluminum-copper (2017Al), and aluminum-silicon-magnesium (SAKG42Al). Plasma transferred arc treatment was carried out with varying amounts of powder and welding currents. The overlay weld layers obtained were then observed to assess the appearance of overlay weld beads, the shape of the beads, and defects. After that, a microstructural analysis of the bead cross section, the extent of melting and solidification, and the dispersion of the NbC particles, was carried out. Based on these results, the range of appropriate welding conditions was established. Niobium carbide particles were then dispersed onto the surface of the samples. The matrix and crystalline phases in the overlay weld alloys were identified using x-ray diffraction (XRD).

2.2 *Corrosion Test and Electrochemical Testing*

An immersion test was carried out by placing the samples in a quiescent 0.5 mol/L NaCl solution open to the air. After the samples were cut into 15 by 15 mm blocks, lead lines were connected to the rear surfaces of the samples using electrically conductive resin. The samples were then placed in epoxy resin, forming the electrode. After that, the surfaces of the samples were sanded with silicon carbide sandpaper, finished with diamond paste (particle size 3 μm), rinsed with acetone, and completely masked with silicone resin, leaving only an electrode area of 10 by 10 mm. Electrodes were then stored for 86.4 ks to allow the resin to harden and were then rinsed with ion exchange water and immersed in the corrosive solution. During the immersion test, the corrosion potentials of the samples were continuously measured using a Ag/AgCl/saturated potassium

chloride electrode (SSE). Potential display conformed entirely to SSE standards, and the testing temperature was 303 K. After the corrosion test, the sample surfaces were rinsed thoroughly, using tap water then ion exchange water. After drying in cool air, the samples were placed in a desiccator. The corroded surfaces were then observed using scanning electron microscopy (SEM), and the elements were analyzed using energy dispersive spectroscopy (EDS). In some cases, corroded samples were lightly polished to observe the changes.

To assess the polarization behavior of the samples in sodium chloride solution, polarization was carried out in the cathodic and anodic directions from the corrosion potential after 0.6 ks of immersion, at a scanning rate of 0.2 mV/s; the current flowing at that time was then measured. As the corrosion potentials were unstable in an aerated solution, a 0.1 mol/L sodium chloride solution through which high-purity argon gas had been passed for 3.6 ks prior to the start of the experiment was used as the corrosive solution. Small amounts of gas were also introduced during the measurement process. Using this approach, potential-current density curves could also be measured with good sample reproducibility.

3. Results and Discussion

3.1 *Microstructure of Overlay Weld Alloys*

Niobium carbide powder was uniformly supplied at a rate of 2.4 kg/s, while the plasma weld current was varied between 60 to 160 A. As shown in Fig. 1, good bead surface shapes were obtained at 90 and 100 A. In the lower levels of the bead cross section, the distribution density of NbC particles was higher. This phenomenon was verified for all aluminum substrates and was due to the fact that the density of the NbC particles was significantly higher than that of the aluminum alloys, causing the NbC particles to settle when the aluminum alloy substrates were in a melted state. Samples for the corrosion test and metallographical examination were cut out of overlay weld layer sections in which NbC particles were dispersed in high densities.

Figure 2(a) shows the distribution of the NbC particles for the overlay weld layers of the various aluminum alloys, and Fig. 2(b) shows the microstructure of the matrix position of these layers. As shown in Fig. 2(a), the NbC particles were distributed uniformly, but minute hemispherical pores were also present in spots. The microstructures of the matrix alloys (Fig. 2b) were as follows: 4NAl was homogeneous, while crystalline phases were verified in 5052Al, 2017Al, and SAKG42Al. The XRD patterns of the overlay weld alloy matrix and crystalline phases for 2017Al are shown as examples in Fig. 3. The diffraction peaks of Al and NbC particles were observed in the matrix, in addition to weak peaks of Al_3Nb and $CuAl_2$. Table 2 shows the identification results of the remainder of the aluminum overlay weld alloys. Niobium carbide particles fused to a part of the surface during overlay welding process, suggesting that they bonded to the aluminum substrate. $CuAl_2$ crystalline phase was verified in 2017Al, while silicon crystalline phase was verified in SAKG42Al.

3.2 *Corrosion Morphologies*

Figure 4 shows the surfaces of the various aluminum overlay weld alloys without dispersion of NbC particles after being immersed for 288 ks in quiescent, 0.5 mol/L NaCl open to the air. 4NAl and 5052Al showed almost no evidence of corrosion nor any accumulation of corrosion products. In the case of 2017Al, indications are present that dissolution occurred in the vicinity of the crystalline phases. According to EDS analysis, these crystalline phases are a composition of aluminum-copper ($CuAl_2$). SAKG42Al was completely covered with a film of corrosion products.

Although not indicated in this paper, the corrosion potentials of overlay weld alloys containing dispersed carbides changed over time as follows: immediately after immersion, SAKG42Al, 5052Al, 4NAl, and 2017Al (in that order) took on negative corrosion potentials; SAKG42Al and 5052Al then moved in a positive direction as immersion progressed. Almost no change was seen in 4NAl and 2017Al, with all overlay weld alloys remaining in the –0.6 to –0.7 V (versus SSE) range after 288 ks of immersion

The morphologies of the alloy surfaces after 288 ks of immersion are shown in Fig. 5. As shown in Fig. 5(a), when NbC particles were dispersed in the various aluminum overlay weld alloys, a spotty accumulation of corrosion products (white part) was noted on all alloys. The matrix sections of 4NAl, 5052Al, and 2017Al were all covered with coatings of corrosion products. Particle-shaped corrosion products covered SAKG42Al, and groove-shaped depressions were visible in the vicinity of the NbC particles. Figure 5(b) shows the form after the accumulated corrosion products were removed from the surface. Groove-shaped traces of dissolution appeared on the NbC particles and crystalline phase-matrix interfaces. Slight corrosion was seen in 4NAl and 5052Al, while marked corrosion was seen in 2017Al and SAKG42Al, which contained large quantities of crystalline phase.

Using EDS, the whisker-shaped crystalline phase of 2017Al was identified as copper-aluminum; the crystalline phase on SAKG42Al was identified as being made up mainly of silicon. This would suggest that overall corrosion of the matrix alloys, crevice corrosion by NbC particles and crystalline phases near

Table 1 Chemical composition of the aluminum alloys

	Composition, mass %								
	Si	Fe	Cu	Mn	Mg	Cr	Zn	Ti	Al
99 99% Al (4NAl)	...	.	...	...	...	...	...	...	...
Al-Mg (5052)	0.11	0 23	0.06	0.03	2.51	0.21	Trace	0.02	bal
Al-Cu (2017)	0 32	0.22	4.07	0.43	0.45	0.01	0 02	0.02	bal
Al-Mg-Si (SAKG42)	7.56	0 15	0.00	0 12	1.90	Trace	0	..	bal

the matrix, and galvanic corrosion caused by contact with foreign substances may all occur simultaneously.

3.3 *Electrochemical Behavior*

Figure 6 shows the polarization behavior of various types of samples when placed in deaerated 0.1 mol/L sodium chloride solution using high-purity argon gas. Substrate 4NAl (Fig. 6a), which did not undergo PTA treatment (virgin), showed corrosion potential in the vicinity of –1.2 V; under anodic polarization, the current started to flow, and a passive current density was shown. After that, the anodic current increased dramatically from –0.6 V, showing pitting potential. On the other hand, the cathodic polarization curve showed that the current increased gradually and increased linearly from around –1.3 V. With PTA-treated 4NAl substrate, the corrosion potential shifted slightly positive, and although the anodic and cathodic currents increased very slightly, this substrate showed similar polarization behavior to almost all untreated materials. For the 4NAl with dispersed NbC particles, corrosion potential shifted greatly in the positive direction, and the anodic current increased immediately and dramatically from corrosion potential. After the slight initial increase, the cathodic current increased in a straight line from –0.8 V. That is to say, the cathodic current of the 4NAl with dispersed NbC particles appeared to be much larger than that of the alloy without dispersed NbC particles.

For 5052Al (Fig. 6b), the corrosion potentials of the untreated and PTA-treated materials were almost identical; the cathodic current increased linearly. Under anodic polarization, after very slight initial passivation, current increased dramatically from –0.4 V due to the generation of localized corrosion. Niobium carbide particles were dispersed with the result that a

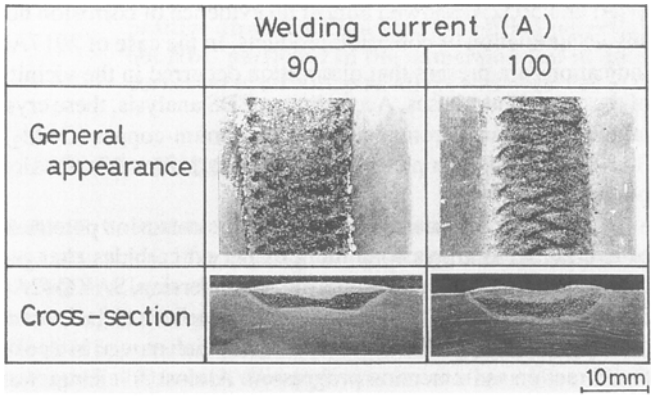

Fig. 1 Microstructures of the weld bead on aluminum alloy with dispersed NbC particles. NbC powder feeding rate is 40 g/min

Table 2 Crystalline materials in aluminum overlay weld alloys with dispersed NbC particles determined by x-ray diffraction method

Alloy	Phase
Al (99.99% Al)	Al, NbC, Al_3Nb
Al-Mg (5052)	Al, NbC, Al_3Nb
Al-Cu (2017)	Al, NbC, Al_3Nb, $CuAl_2$
Al-Mg-Si (SAKG42)	Al, NbC, Al_3Nb, Si

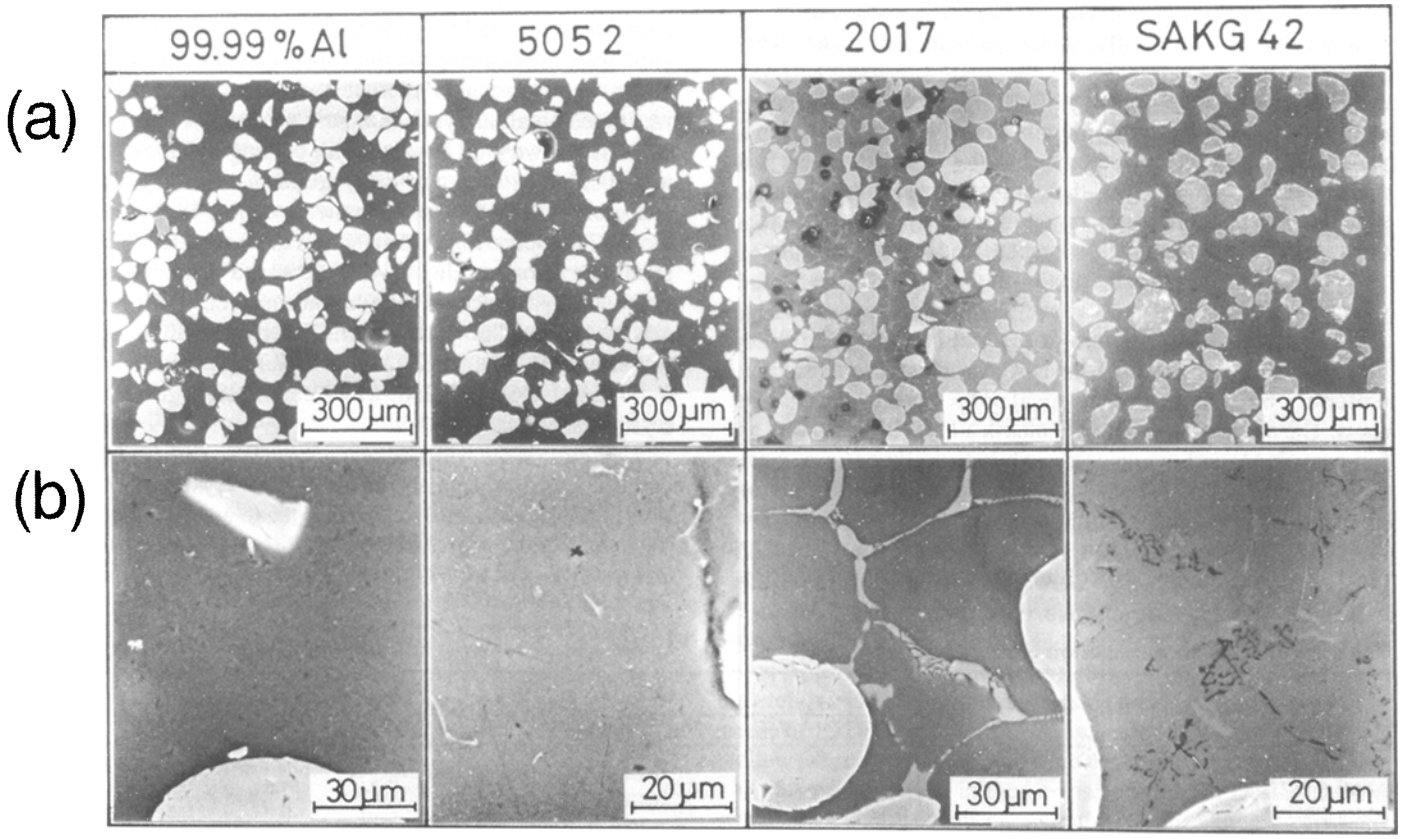

Fig. 2 Microstructures of aluminum overlay weld alloys with dispersed NbC particles (a) Distribution of NbC particles. (b) Matrix area

slightly positive corrosion potential was created. The anodic current increased linearly; for in cathodic current, a slight initial stagnation was followed by a linear increase.

In the case of 2017Al (Fig. 6d), the corrosion potential was less negative than that of 4NAl; changes to anodic and cathodic current resulting from the dispersion of NbC particles were almost equal. That is to say, the cathodic current from the corrosion potential increased gradually at first, but a dramatic linear increase then followed. Under anodic polarization, a slight passive region was observed, and current then increased dramatically from –0.5 V.

SAKG42Al (Fig. 6c) had the lowest corrosion potential for any of the untreated materials. A straight-line increase of cathodic current from the corrosion potential was observed. Under anodic polarization of SAKG42Al, an even constant current density of 5×10^{-2} A/m^2 (passive region) was observed between the corrosion potential and pitting potential, and the current increased dramatically from –0.5 V. The same trend was observed without dispersed NbC particles, and the corrosion potential of SAKG42Al with dispersed NbC particles shifted slightly higher to –1.0 V, and the cathodic current rose dramatically. Under anodic polarization, after displaying passive current density, current increased dramatically from –0.5 V.

Thus, the localized corrosion potentials of all aluminum alloys with dispersed NbC particles in deaerated 0.1 mol/L NaCl solution were approximately –0.6 V, which is the same value seen for specimens without the NbC particle dispersion.

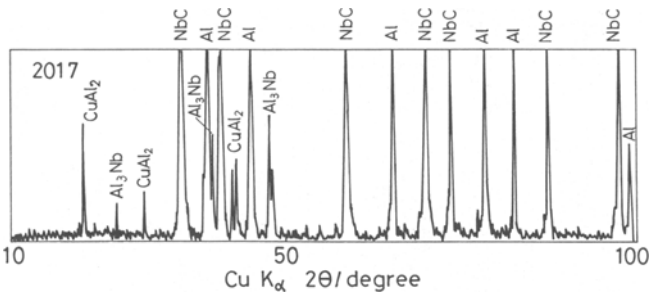

Fig. 3 X-ray diffraction pattern of 2017 aluminum overlay weld alloys with dispersed NbC particles

3.4 *Corrosion Behavior of Overlay Weld Alloys*

Aluminum overlay weld alloys, 2017Al and 5052Al (Fig. 6) showed almost identical polarization behavior whether untreated, PTA-treated, or NbC-dispersed alloys were used, meaning that no effect from PTA treatment or dispersion of NbC particles could be verified.

The 2017Al and 5052Al matrices possessed slightly more positive corrosion potentials than the other alloys, approaching the corrosion potential of NbC particles. However, NbC particles were stable in sodium chloride solution (Ref 13). The 2017Al and 5052Al matrices and the NbC particles, which are electrochemically similar, were covered by a thin passivating film, and the solubility of these films is thought to determine the corrosion resistance of the carbide-dispersed overlay weld alloys.

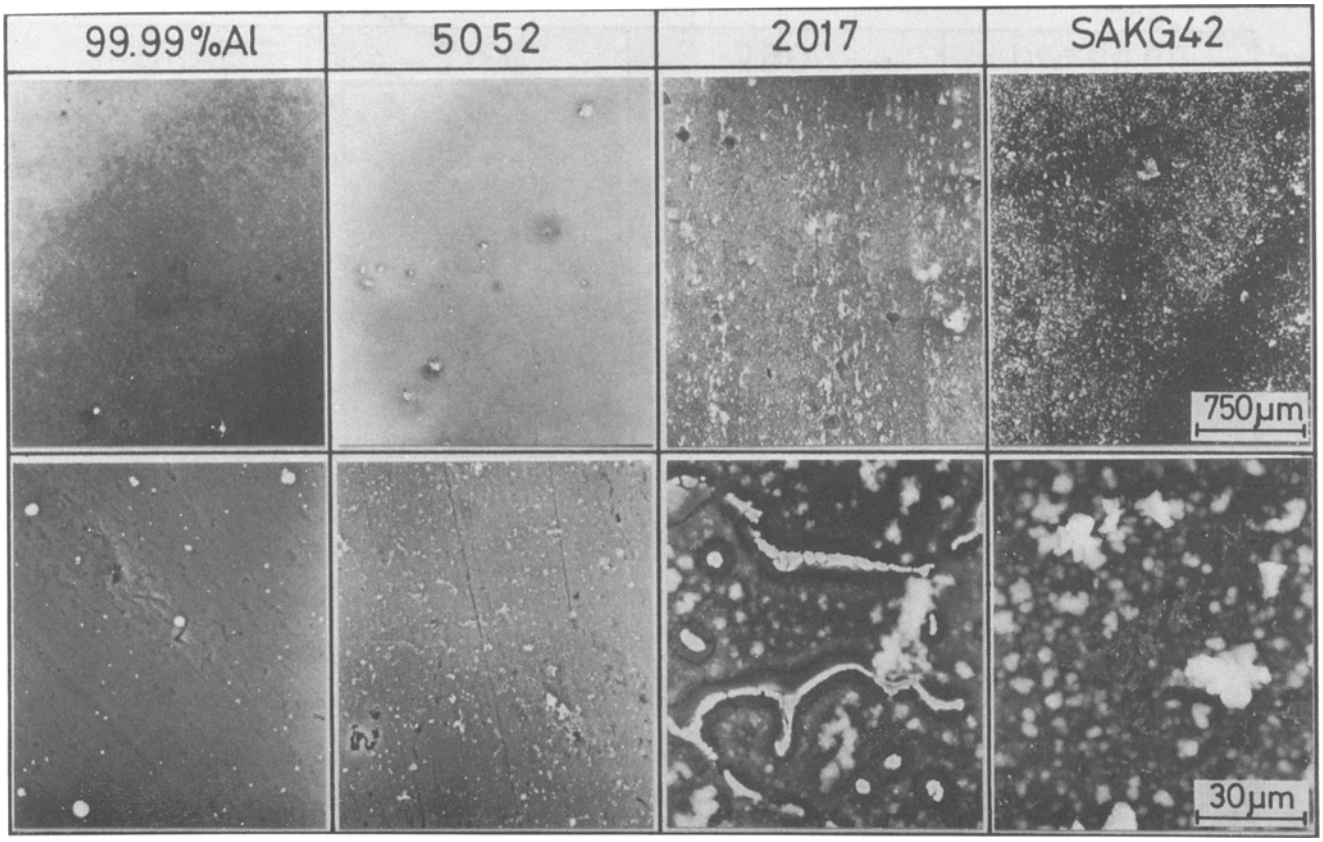

Fig. 4 Scanning electron micrographs of the corrosion surface of aluminum overlay weld alloys without dispersed NbC particles after immersion testing during 288 ks in open-to-air 0 5 mol/L NaCl solution at 303 K

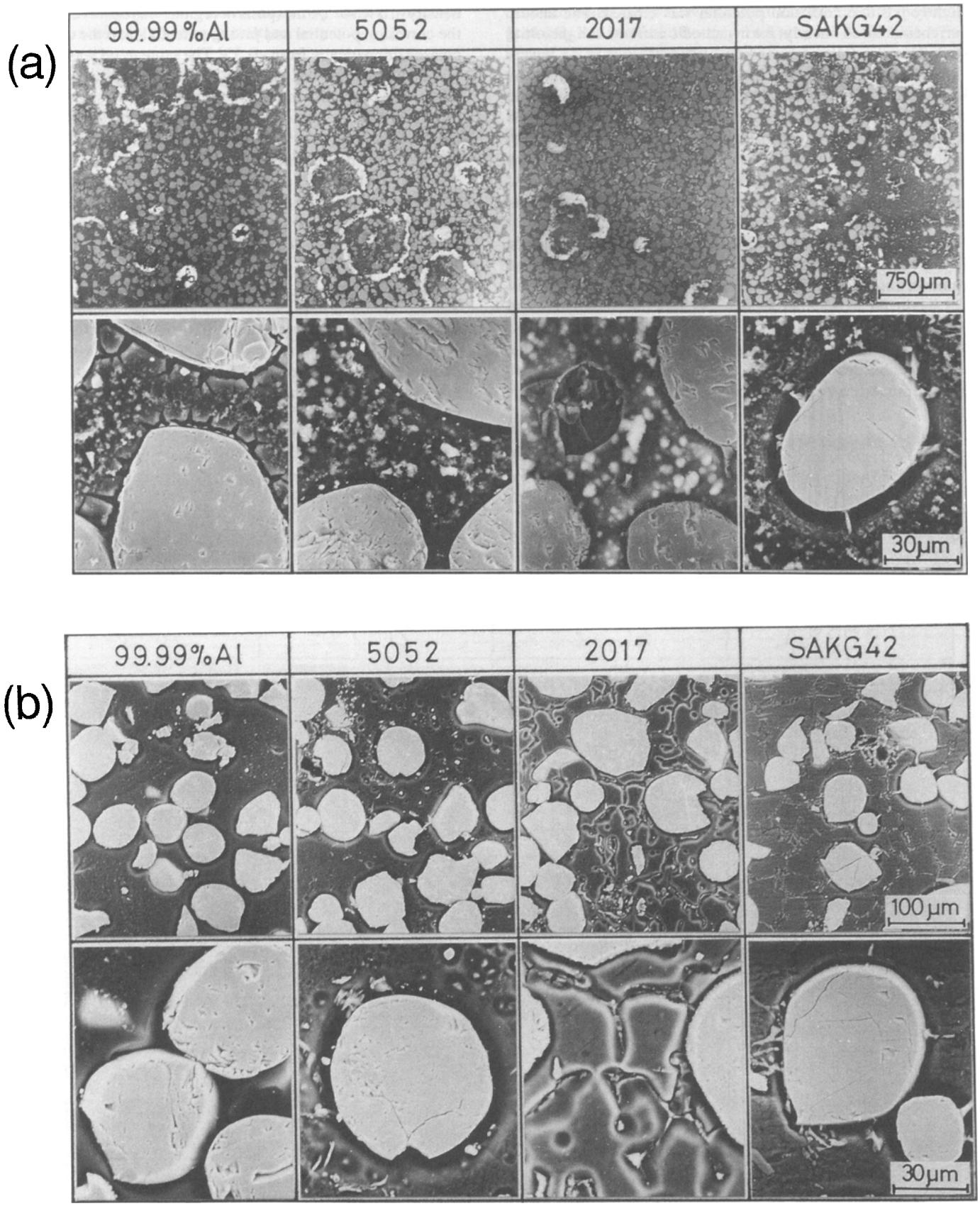

Fig. 5 Scanning electron micrographs of the corrosion surface on aluminum overlay weld alloys with NbC particles after immersion test during 288 ks in open-to-air 0.5 mol/L NaCl solution at 303 K. (a) After rinsing in distilled water (b) After repolishing

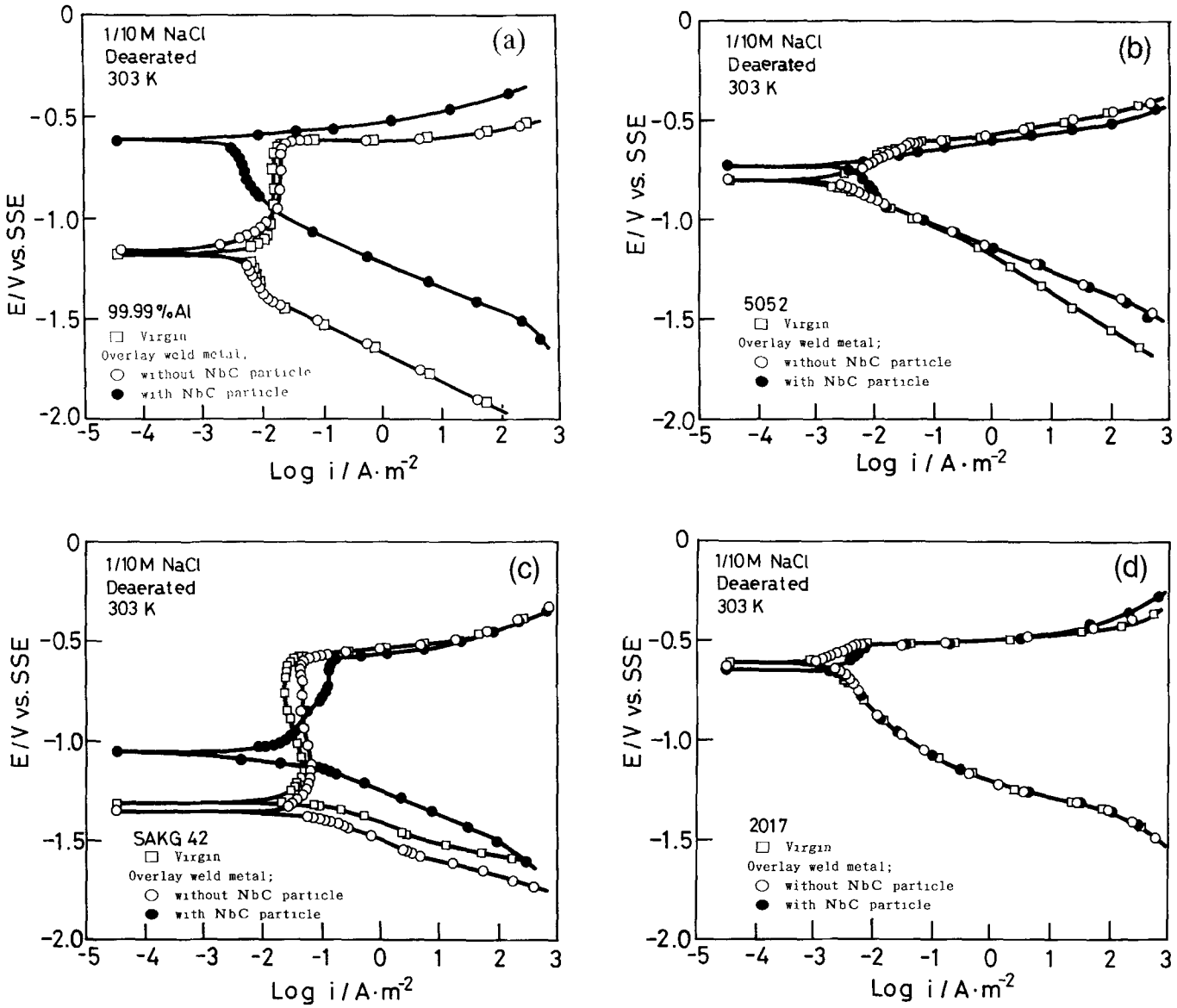

Fig. 6 Polarization curves of aluminum alloys without and with dispersed NbC particles in deaerated 0.1 mol/L NaCl solution at 303 K. (a) Pure Al. (b) Al-Mg (5052) (c) Al-Mg-Si (SAKG42). (d) Al-Cu (2017)

Untreated 4NAl and SAKG42Al both possessed extremely negative corrosion potentials, and passive current density was observed over a wide potential range until the localized corrosion potential was reached. As a result of dispersed NbC particles, the corrosion potential shifted in a positive direction, but localized corrosion potential remained almost unchanged. Under cathodic polarization, a hydrogen-evolution current was realized immediately.

This tendency was almost unchanged in PTA-treated alloys, and the localized corrosion potential also remained almost unchanged. However, with dispersed-NbC particles, the cathodic reaction became much stronger while the corrosion potential of the overlay weld alloy was situated within the passive potential range.

These findings imply that the NbC particles polarize the aluminum matrix into the anode. In addition, the start-up potential of the cathodic current was located in the potential range in which the hydrogen evolution reaction occurs (Ref 14). Consequently, it seems that, in aqueous solution, the cathodic reduction reaction progresses on the particle surfaces of aluminum overlay weld alloys with dispersed NbC particles, and while the aluminum matrix dissolves, the reaction that forms a passivating film progresses. As with aluminum-magnesium-silicon (SAKG42Al), the large potential difference between carbide particles and the matrix leads to the galvanic corrosion reaction so that the matrix dissolved fiercely into grooves in the vicinity of the NbC particle interface (Fig. 5).

4. Conclusions

The 4NAl, 5052Al, and 2017Al overlay weld alloys yielded matrix surfaces covered with thin films of corrosion products, while the NbC particles remained unaffected. The SAKG42Al

matrix alloy corroded. In all overlay weld alloys with dispersed NbC particles, the matrix alloys dissolved into groove shapes at the matrix interface between the crystalline phases and the NbC particles. This tendency was most marked in 2017Al and SAKG42Al.

In terms of anodic polarization characteristics, 5052Al and 2017Al showed little difference whether the alloys were untreated (i.e., no PTA treatment with dispersed NbC particles) or treated with dispersed NbC particles. When untreated, SAKG42Al showed extremely negative corrosion potential; with dispersed NbC particles, it showed only slight movement in the positive direction and a large passive current density range. However, PTA treatment or NbC-particle dispersion hardly affected their localized corrosion potentials at all. For 4NAl, PTA treatment exerted minimal influence on anodic polarization characteristics, while dispersion with NbC particles caused corrosion potential to move in a positive direction, approaching the localized corrosion potential, and an immediate rise in anodic current was observed.

References

1 F. Matsuda, Present Situation and Probability of the Forming Technology of a Thick and Hard Layer on Aluminum, *J. Jpn. Inst. Light Met.*, Vol 40 (No. 10), 1990, p 746-752

2 T. Tomita, Y. Takatani, and Y. Harada, Composite Alloying of Metal Surface by Plasma Transferred Arc Welding Process, *Mater. Jpn.*, Vol 31 (No. 12), 1992, p 1056-1063

3. S. Shimizu, K Nagai, F Matsuda, and K. Nakata, Carbide Addition on Aluminum Alloy Surface by Plasma Transferred Arc Welding Process, *J. Jpn. Inst. Light Met.*, Vol 40 (No 10), 1990, p 761-767

4 F. Matsuda, K. Nakata, S. Shimizu, and K. Nagai, Carbide Addition on Aluminum Alloy Surface by Plasma Transferred Arc Welding Process, *Trans. JWRI*, Vol 19 (No. 2), 1990, p 241-247

5. A. Ohkura, *Fundamentals of Advanced Materials*, K Komai, Ed., Ohomu, Tokyo, 1991, p 59-64

6. P.P. Trzaskoma and E. McCafferty, Corrosion Behavior of SiC/Al Metal Matrix Composites, *J. Electrochem. Soc.*, Vol 130 (No 9), 1983, p 1804-1809

7. D.M. Aylor and P J. Moran, Effect of Reinforcement on the Pitting Behavior of Aluminum-Base Metal Matrix Composites, *J. Electrochem. Soc.*, Vol 132 (No 6), 1985, p 1277-1281

8. H. Sun, E.Y. Koo, and H.G. Wheat, Corrosion Behavior of SiCp/6061 Al Metal Matrix Composites, *Corrosion*, Vol 47 (No 10), 1991, p 741-753

9. J Dutta, L.R. Elkin, and J.D. King, Corrosion Behavior of a P130x Graphite Fiber Reinforced 6063 Aluminum Composite Laminate in Aqueous Environments, *J. Electrochem. Soc.*, Vol 138 (No. 11), 1991, p 3199-3209

10. Y. Shimizu, T. Nishimura, and M. Tamura, Corrosion Performance of Al-Base Metal-Matrix-Composites (MMC), *Corros. Eng. Jpn.*, Vol 40 (No. 6), 1991, p 406-412

11. K. Noda, H. Ono, T. Thuru, H Tezuka, and A. Kamio, Pitting Corrosion Behavior of SiC/Al Alloy Matrix Composites, *J. Jpn. Inst. Met.*, Vol 56 (No. 6), 1992, p 641-647

12. K Minoshima, Report of Corr. Eng Division, *Soc. Mater. Sci. Jpn.*, Vol 31 (No. 168), 1992, p 1-18

13 Y. Takatani, T Tomita, and Y Harada, Corrosion Behavior of Carbides in Sodium Chloride Solution, *J. Soc. Mater. Sci. Jpn.*, Vol 41 (No 468), 1992, p 1348-1353

14 M Pourbaix and N. De Zoubov, *Atlas of Electrochemical Equilibria in Aqueous Solutions*, M Pourbaix, Ed , National Association of Corrosion Engineers, 1974, p 97-105